Identification of C-terminal hydrophobic residues important for dimerization and all known functions of ParB of *Pseudomonas aeruginosa*

Mierzejewska, J.[1#], Bartosik, A. A.[1], Macioszek, M.[1], Płochocka, D.[1], Thomas, C.M.[2] and Jagura-Burdzy, G.[1]*

[1] The Institute of Biochemistry and Biophysics, PAS, 02-106 Warsaw, Pawinskiego 5A, Poland

[2] School of Biosciences, The University of Birmingham, Edgbaston, Birmingham, B15 2TT, UK.

[#]Present address: Institute of Biotechnology, Faculty of Chemistry, Warsaw University of Technology, Warsaw, Noakowskiego 3, Poland.

*Author for correspondence:
The Institute of Biochemistry and Biophysics, PAS, 02-106 Warsaw, Pawinskiego 5A, Poland,
Tel: +48 22 823 71 92
Fax: +48 22 658 46 36
Email: gjburdzy@ibb.waw.pl

Running title: Dimerization domain of ParB

Key words: ParB; *Pseudomonas aeruginosa*; dimerization, C-terminus

Abbreviations: DAPI, 4',6-diamidino-2-phenylindole

ABSTRACT

The ParB protein of *P. aeruginosa* is important for growth, cell division, nucleoid segregation and different types of motility. To further understand its function we have demonstrated a vital role of the hydrophobic residues in the C-terminus of $ParB_{P.a}$. By *in silico* modeling of the C-terminal domain (242-290 amino acids) the hydrophobic residues L282, V285 and I289 (but not L286) are engaged in leucine zipper-like structure formation, whereas the charged residues R290 and Q266 are implicated in forming a salt bridge involved in protein stabilization. Five *parB* mutant alleles were constructed and their functionality defined *in vivo* and *in vitro*. In agreement with model predictions the substitution of L286A had no effect on mutant protein activities. Two ParBs with single substitutions of L282A or V285A and deletions of two or seven C-terminal amino acids were impaired in both dimerization and DNA binding and were not able to silence genes adjacent to *parS* suggesting that dimerization through the C-terminus is a prerequisite for spreading on DNA. The defect in dimerization also correlated with loss of ability to interact with partner protein ParA. Reverse genetics demonstrated that a *parB* mutant producing ParB lacking the two C-terminal amino acids as well as mutants producing ParB with single substitution L282A or V285A had defects comparable to those of a *parB null* mutant. Thus so far all the properties of ParB seem to depend on dimerization.

INTRODUCTION

The essential role of *par* loci in plasmid partitioning has long been appreciated (Williams & Thomas, 1992), while the function of chromosomally encoded *par* loci in the segregation of bacterial chromosomes is less clear. The chromosomally encoded *par* loci are highly conserved and belong to Type I partitioning systems (Gerdes *et al.*, 2000). Besides the high level of identity in amino acid sequences of the chromosomal homologues of ParA and ParB, the *parS* sequences are also extremely well conserved at least between so called primary chromosomes. The localization of the *parAB* genes, as well as the majority of *parS* sites, in close vicinity to the *oriC* region could indicate a role of *par* systems in replication/segregation of chromosomes, as genes known to be crucial for these processes are situated within the *oriC* domain (20% of chromosome around *oriC*). Moreover the chromosomal *par* systems are able to promote active segregation and stabilization of otherwise unstable replicons even in heterologous host cells (Bartosik *et al.*, 2004; Godfrin-Estevenon *et al.*, 2002; Lin & Grossman, 1998; Yamaichi & Niki, 2000). Although these features of chromosomally-encoded *par* loci might suggest that they should play a similar biological function in chromosome segregation as plasmid *par* systems play for plasmid DNA, studies on *par* mutants in different bacteria have revealed a more complex picture. With the exception of *Caulobacter crescentus*, the chromosomal *parA parB* genes are not essential for cell viability (Mohl & Gober, 1997). However, mutations in the *parA* (*soj*) and *parB* (*spo0J*) genes lead to defects in the sporulation of *Bacilus subtilis* (Cervin *et al.*, 1998; Quisel *et al.*, 1999; Quisel & Grossman, 2000), *Streptomyces coelicolor* (Jakimowicz *et al.*, 2002; 2006; 2007; Kim *et al.*, 2000) and in vegetative chromosome partitioning of *B. subtilis* (Ireton *et al.*, 1994), *Pseudomonas aeruginosa* (Lasocki *et al.*, 2007; Bartosik *et al.*, 2009) and *Pseudomonas putida* (Lewis *et al.*, 2002; Godfrin-Estevenon *et al.*, 2002). Several studies have implicated a role for *par* genes in origin localization and segregation (Bowman *et al.*, 2008; Ebersbach *et al.*, 2008; Figge *et al.*, 2003; Fogel & Waldor, 2006; Glaser *et al.*, 1997; Jakimowicz *et al.*, 2007; Lee *et al.*, 2003; Ptacin *et al.*, 2010; Saint-Dic *et al.*, 2006; Sharpe & Errington, 1996; Toro *et al.*, 2008; Viollier *et al.*, 2004), in the separation of sister origins and in the regulation of replication (Kadoya *et al.*, 2011; Lee & Grossman, 2006; Murray & Errington, 2008; Ogura *et al.*, 2003; Scholefield *et al.*, 2011; Webb *et al.*, 1997), SMC recruitment to the nucleoid (Gruber & Errington, 2009; Sullivan *et al.*, 2009) or in cell division initiation and cell cycle coordination (Autret & Errington, 2003; Figge *et al.*, 2003; Jakimowicz *et al.*, 2007; Marston & Errington, 1999; Mohl *et al.*, 2001; Real *et al.*, 2005; Schofield *et al.*, 2010; Thanbichler & Shapiro, 2006).

In *P. aeruginosa*, a facultative pathogen, the *par* locus has been identified ~8 kb from *oriC*, eight out of ten *parS* sequences are located in the *ori* domain. The ParABS system of *P. aeruginosa* can stabilize an unstable plasmid in *E. coli* (Bartosik *et al.*, 2004). Neither ParA nor ParB of *P. aeruginosa* are essential for the viability of the cells. Their lack causes visible phenotypic defects (more severe in the *parA* mutant) which include a >200 fold increase in the number of anucleate cells, longer cells, slower growth rate and perturbations in colony formation and motilities (Bartosik *et al.*, 2009; Lasocki *et al.*, 2007). The increased frequency of chromosome loss observed in actively dividing cells of a *P. aeruginosa parB* mutant (Bartosik *et al.*, 2009) has been also reported for *P. putida parB* (Godfrin-Estevenon *et al.*, 2002; Lewis *et al.*, 2002) mutants, but only in transient and stationary phase of culture growth. The other phenotypical defects (motilities defects, changed colony morphology, increase in cell size) caused by the lack of $ParB_{P.a.}$ seem to be unique among ParB representatives and so far unexplained.

In terms of molecular functions previous studies (Bartosik *et al.*, 2004) showed that ParB protein of *P. aeruginosa* conforms to behavior of other chromosome- and plasmid-encoded homologues. It demonstrates ability: to interact with ParA; to dimerize and to bind centromere-like sequences (*parS*). $ParB_{P.a.}$ has the ability to spread on DNA and silence genes adjacent to the *parS* sites and it has been shown that this effect is dependent on a putative H-T-H motif, the ability of ParB to dimerize, and also on an intact N-terminus (Bartosik *et al.*, 2004; Kusiak *et al.*, 2011). ParB also forms regularly distributed foci in *P. aeruginosa* cells which co-localize with the nucleoid and undergo dynamic changes (Bartosik *et al.*, 2009). In this study, we dissected the C-terminus of ParB from *P. aeruginosa* demonstrating the vital role of the hydrophobic residues and C-tip of the protein in dimerization and all known functions of this protein.

METHODS

Bacterial strains and growth conditions

Escherichia coli strains used were DH5α[F^-(*Φ80*d*lacZΔM15*) *recA1 endA1 gyrA96 thi-1 hsdR17*($r_k^-m_k^+$) *supE44 relA1 deoR Δ(lacZYA-argF)U196*], BL21 F^- *ompT hsdS*$_B$ ($r_B^-m_B^-$) *gal dcm* (λ DE3) (Novagen Inc), BTH101 F^-, *cya-99 araD139 galE15 galK16 rpsL1* (Sm^R) *hsdR2 mcrA1 mcrB1* (Karimova *et al*., 1998) and S17-1 (*pro hsdR hsdM recA* Tp^R Sm^R ΩRP4-Tc::Mu-Km::Tn7) (Simon *et al*., 1986). *Pseudomonas aeruginosa* strains used were PAO1161 (*leu*$^-$, *r*$^-$, *m*$^+$), kindly provided by B.M. Holloway (Monash University, Clayton, Victoria, Australia) and its derivatives - PAO1161 Rif^R (Lasocki *et al.*, 2007), PAO1161 Rif^R *parB1-18*::Tc^R (*parB* null) (Bartosik *et al.*, 2009), PAO1161 Rif^R *parB1-288*, PAO1161 Rif^R *parB1-283*, PAO1161 Rif^R*parB282* and PAO1161 Rif^R*parB285* (all this work).

Bacteria were grown in L broth (Kahn *et al*., 1979) at 37 ^oC or 30 ^oC or on L agar (L broth with 1.5 % w/v agar) supplemented with antibiotics as appropriate: benzyl penicillin sodium salt at 150 μg ml^{-1} in liquid medium and 300 μg ml^{-1} on agar plates for penicillin resistance in *E. coli*, kanamycin sulphate at 50 μg ml^{-1} for kanamycin resistance in *E. coli*, carbenicillin at 300 μg ml^{-1} for carbenicillin resistance in *P. aeruginosa*, rifampicin at 300 μg ml^{-1} for rifampicin resistance in *P. aeruginosa*. Some experiments were performed in M9 minimal medium (Sambrook *et al*., 1989) and on MacConkey Agar Base (Difco) supplemented with 1 % maltose. The L agar used for blue/white screening contained 0.1 mM IPTG and Xgal at 40 μg ml^{-1}.

Plasmid DNA isolation, analysis, cloning and manipulation of DNA

Plasmid DNA was isolated and analyzed by standard procedures (Sambrook *et al*., 1989). The plasmids used in this study are listed in Table 1. Standard PCR (Mullis *et al.*, 1986) was performed as described previously (Lasocki *et al.*, 2007) with the primers listed in Table S1. PCR site-directed mutagenesis (modified method of Stratagene - QuikChange Site-Directed Mutagenesis) was used to make *parB* alleles producing ParBs with single amino acid substitutions - L282A, V285A, L286A. In this procedure supercoiled double stranded plasmid DNA with *parB*$_{P.a}$ (either pKLB2 or pKLB2.8) and pairs of synthetic oligonucleotide primers #21 and #22, #23 and #24, #25 and #26 containing desired mutation (Table S1) were used. The mutagenic oligonucleotide primers were designed to either introduce or remove the restriction site. The plasmid DNA was sequenced to verify the presence of the mutation.

Bacterial transformation

Competent cells of *E. coli* were prepared by standard $CaCl_2$ method (Sambrook *et al*., 1989).

Transformation of *P. aeruginosa* strains was done according to previously published method (Irani & Rowe, 1997).

Introduction of *par* mutant alleles into *P. aeruginosa* PAO1161

Mutant *parB* alleles were cut out as EcoRI-SalI fragments from pMMB5.2, pMMB6.2, pJMB101, pJMB101.1 and inserted into pAKE600, suicide vector unable to replicate in *P. aeruginosa* strains (El-Sayed *et al*., 2001), to create pJMB400 pJMB401, pJMB404 and pJMB405, respectively. To provide the region of homology downstream of truncated *parB*s the 389 bp DNA fragment corresponding to genomic DNA adjacent to 3' end of *parB* was PCR amplified with the pair of primers #11 and #12 (Fig. S1) and then introduced as a SalI-BamHI fragment into pJMB400, pJMB401, pJMB404, and pJMB405 to form pJMB402, pJMB403, pJMB406, and pJMB407, respectively.

Transformants of *E. coli* strain S17-1 with pAKE600 derivatives were used as the donors in conjugation with the recipient strain *P. aeruginosa* PAO1161Rif^R. The transconjugants with pAKE600 derivatives integrated into the chromosome were treated as described previously (Lasocki *et al*., 2007). The PCR products (chromosomal DNA isolated from the putative mutants as the templates with primers #1 and #12) were screened by SalI digestion and finally the presence of modifications was confirmed by sequencing of PCR fragments.

"Silencing" assay

E. coli DH5α(pABB811*parS*$_{2/3I}$) and DH5α(pGB2) cells were transformed with the appropriate pGBT30*tacp-parB* derivatives. Undiluted and the 10-, 100- fold dilutions of the initial transformation mixture were plated to select for incoming plasmid (L agar supplemented with penicillin) or both for incoming and resident plasmid (L agar with penicillin and streptomycin) with and without 0.5 mM IPTG to induce ParB production. After 24 h incubation at 37 °C the colonies were counted and the number of different class transformants in the original transformation mixture was estimated.

Purification of His$_6$-tagged proteins

E. coli strain BL21(DE3) was transformed with pET28mod derivatives encoding histidine-tagged (MGSS*HHHHHH*SSGLVPRGSHSEF) ParB derivatives and protein over-expression and purification was carried out as described before (Bartosik *et al.*, 2004).

Cross-linking with glutaraldehyde.

His$_6$-tagged polypeptides purified on Ni^{2+}-agarose columns (at conc. 0.1 mg ml^{-1}) were cross-linked by use of glutaraldehyde (Jagura-Burdzy & Thomas, 1995) and separated on 10 % (w/v) SDS-PAGE gels. The proteins were transferred onto nitrocellulose membrane and

Western blot analysis was performed with anti-ParB antibodies, as described previously (Bartosik *et al.*, 2004).

Analysis of protein-DNA interactions by electrophoretic mobility shift assay (EMSA)

To check the ability of mutated $ParB_{P.a}$ proteins to bind *parS* DNA *in vitro*, the nonradioactive electrophoretic mobility shift assay (Leonard *et al.*, 2004) was performed. A 16 bp dsDNA fragment (annealed oligonucleotides, #17 and #18, Table S1) containing the $parS_{2/3}$ (Bartosik *et al.*, 2004) was used in EMSA. 5.6 pmoles of $parS_{2/3}$ oligonucleotides without or with increased concentration of purified His_6-tagged ParB and its derivatives were incubated at conditions described previously (Kusiak *et al.*, 2011). Negative control of the binding reaction was provided by use of unrelated dsDNA with palindromic sequence (annealed primers #19 and #20, Table S1) and the same amounts of ParB in the incubation mixture. The samples were analyzed on 10% (w/v) non-denaturing polyacrylamide gel in TBE buffer (Sambrook et al., 1989). DNA bands were stained with 0.5 μg ethidium bromide ml^{-1} and visualized on a UV transilluminator.

Growth experiments and sample preparation for Western blotting

The growth of bacteria was monitored by measuring the optical density at 600 nm (OD_{600}); the cultures were diluted and plated on L agar to establish c. f. u. ml^{-1}. Bacteria were harvested, resuspended in sonication buffer (50 mM phosphate buffer; pH 8.0 and 300 mM NaCl) and disrupted by sonication. Crude extracts from the same number of cells were analyzed by SDS-PAGE followed by Western blotting performed as described previously (Bartosik *et al.*, 2004).

Bacterial Adenylate Cyclase Two-Hybrid System (BACTH system)

The interactions between ParB mutant derivatives and either WT ParB or ParA were analyzed using the bacterial two-hybrid system BACTH (Karimova *et al.*, 1998). The C-terminal *parB* mutant alleles have been cloned as EcoRI-HincII fragments from pET28mod derivatives into pLKB4 (derivative of pUT18C) to create translational fusions with the T18 catalytic domain of *Bordetella pertussis* adenylate cyclase – CyaT18-ParB. The wt *parA* and wt *parB* alleles have been cloned into pLKB2 (modified pKT25) to produce translational fusions: CyaT25-ParA and CyaAT25-ParB. *E. coli* BTH101 *cya* strain was co-transformed with both pLKB4 and pLKB2 derivatives and plated on indicator MacConkey base medium supplemented with 1% maltose (as the only carbon source), penicillin, kanamycin and 0.5 mM IPTG. The plates were incubated for 48 h at 27 °C.

Motility assays

The swimming and swarming and twitching assays were performed according to Rashid & Kornberg, (2000) with modifications described previously (Lasocki *et al.*, 2007). All sets of plates were standardized by using the same volume of medium.

DAPI staining and immunofluorescence microscopy

The DAPI staining procedure and immunofluorescence microscopy was carried out as previously described (Bartosik *et al.*, 2004; Bignell *et a*l., 1999). Cells were examined using an Eclipse E800 light fluorescence microscope (Nikon) fitted with an ORCA ER CCD camera (Hamamatsu). Images were captured and manipulated on PC Windows XP Professional PL with the Lucia General 5.0 (Laboratory Imaging).

In silico $ParB_{P.a.}$**dimer modeling**

Amino acids sequences of ParB of *P. aeruginosa*, ParB of *P. putida*, KorB of RK2/RP4 (IncP-1α) and R751 (IncP-1β) were aligned using MAFT (Katoh & Toh, 2008), CLUSTALW (Larkin *et al.*, 2007) and T-Coffee (Notredame, 2000) servers, and manually adjusted. Structural model of monomeric C-terminus of *P. aeruginosa* ParB was obtained using Sybyl-x1.1 package (TRIPOS, USA) on the basis of $ParB_{P.a.}$ and $KorB_{RP4}$ alignment (Fig. S2) and $KorB_{RP4}$ crystal structure (Delbruck *et al.*, 2002). Structure of the C-terminal dimer of $ParB_{P.a.}$ (superposition on KorB dimer) was subjected to energy minimization (100 steps) using the AmberFF99 force field as implemented in Sybyl-x1.1.

RESULTS

Predicting amino acids essential for ParB dimerization

A comparison of $ParB_{Pa}$ (290 amino acids) with other chromosomal homologues revealed highly conserved segments designated BoxI (S66-R79) and BoxII (Y86-A97) (Yamaichi & Niki, 2000), a H-T-H motif and regions 1 to 4 (R6-L16, L123-A138, V211-L224, G270-I289, respectively) (Bartosik *et al.*, 2004) (Fig. S1). Previous studies on $ParB_{Pa}$ using *in vivo* and *in vitro* methods (Bartosik *et al.*, 2004) identified a C-terminal fragment of 56 amino acids (ParB235-290) as the dimerization domain for $ParB_{Pa}$ and indicated that deletion of the last seven residues from this domain (ParB235-283) abolished its dimerization. The three-dimensional structure of $ParB_{Pa.}$ has not yet been solved. The sequence of the C-terminus of $ParB_{Pa}$ aligns well with C-terminal part of ParB homologue – KorB of RK2 (IncP-1α) (Fig. S2) and moreover the two domains are functionally interchangeable. Replacement of 61 amino acids from the C-terminus of ParB by the C-terminal 100 amino acids of KorB (ParB1-229-KorB258-358) restores its ability to dimerize and bind *parS* with high affinity *in vitro* as well as to transcriptionally silence genes near a *parS* site *in vivo* (Bartosik *et al*., 2004). Therefore on the basis of crystallographic analysis of the C-terminal part of KorB of RK2/RP4 (Delbrück *et al*., 2002) a model of C-terminal domain of $ParB_{Pa.}$ was built *in silico* (Fig. 1). According to this model the hydrophobic residues L282, V285 and I289 (but not L286) are engaged in a leucine zipper-like structure, whereas the charged R290, and Q266 are implicated in forming a salt bridge involved in stabilization of the ParB dimer. To verify this model, two alleles of *parB* with C-terminal deletions of either seven amino acids (*parB1-283*) or two amino acids, I289 and R290, (*parB1-288*) were PCR-amplified and three alleles coding for ParBs with single amino acid substitution - L282A, V285A and L286A were constructed by applying PCR site-directed mutagenesis. These alleles were introduced into appropriate vectors and their products tested for the ability to dimerize, bind DNA *in vitro*, spread on DNA and interact with ParA *in vivo*.

Spreading on DNA *in vivo* – "silencing test" in *E. coli*

The $ParB_{Pa}$ protein recognizes the *parS* sequence as a dimer, then self-associates and spreads on DNA causing transcriptional silencing of genes adjacent to *parS* (Bartosik *et al*., 2004). The plasmid pGB2 (Churchward *et al.*,1984) used for the "silencing test" is a Sm^R stable replicon based on pSC101 in which an MCS is inserted approximately 200 bp upstream of the promoter for the initiator gene *repA*. The presence of *parS* close to the *repA* promoter in pABB811 does not influence plasmid stability unless WT ParB is produced *in trans* from pKLB2 (*tacp-parB*) (Bartosik *et al*., 2004). The transformation frequency of *E. coli*

DH5α(pABB811) with pKLB2 in the absence of IPTG with selection for incoming and resident plasmid was 2-3 fold lower than the transformation frequency when only the incoming plasmid is selected. Addition of 0.5 mM IPTG to transformation plates with double selection (conditions of ParB overproduction) decreases the number of transformants more than 100-fold (Table 2) in comparison to the number of transformants grown on double selection plates without IPTG.

The silencing test was repeated to establish the effect of overproducing the modified ParB proteins on the stability of pABB811 in *E. coli* DH5α(pABB811). The number of transformants with selection either for incoming plasmid (Pn), or for both incoming and the resident plasmids (Pn Sm) with and without IPTG present are shown in Table 2. Only ParBL286A (pJMB602) caused significant instability of pABB811 and a loss of streptomycin resistance of the recipient strain when ParB was over-produced during growth with IPTG (more than 100-fold decrease in the number of transformants on Pn Sm IPTG plates, effect observed for WT ParB delivered from pKLB2). The other plasmids tested had very little impact on stability of pABB811 (2-3 fold decrease in the number of double transformants grown in the presence of inducer in comparison to the number of transformants selected for incoming plasmid). The deletions of seven (pJMB604) or two amino acids I289 and R290 from the C-terminus (pJMB603) as well as the single amino acid substitutions V285A or L282A impaired the silencing property of ParB. Western blotting on extracts from analyzed transformants has shown level of ParB over-production for all mutant derivatives comparable to WT ParB (Fig. S3).

ParB$_{P.a.}$ dimerization *in vitro*

For the *in vitro* analysis, WT ParB as well as modified ParB proteins [ParB1-283, ParB1-288, ParBL282A, ParBV285A and ParBL286A] with a His$_6$-tag attached to the N-terminus were expressed upon induction with IPTG from pET28mod derivatives in *E. coli* strain BL21(DE3). All ParB variants were present in the soluble cellular fraction and it was possible to purify them in a native form on a Ni^{2+}-agarose column. Wild type ParB$_{P.a.}$ protein was previously found to dimerize and form higher order complexes *in vitro* (Bartosik *et al.*, 2004). The dimerization and oligomerization domains are separate in ParB$_{P.a.}$ (Kusiak *et al.*, 2011). The purified His$_6$-tagged ParB derivatives were treated with increasing concentrations of the cross-linking agent glutaraldehyde (GA). Wild type ParB protein dimerized so strongly that even at the lowest glutaraldehyde concentration (0.001 %) dimeric species were visible. The monomeric and dimeric forms were predominant after SDS-PAGE separation and Coomassie Blue staining (not shown). To visualize higher order complexes, a Western blot

analysis was performed with anti-ParB antibodies (Fig. 2a). ParBL286A dimerized and formed higher order complexes as efficiently as the wild type protein. ParBL282A and ParBV285A dimerized but with much lower effectiveness than WT ParB. The C-truncated ParBs – ParB1-283 and ParB1-288 were drastically impaired in dimerization. These results confirmed that the C-terminal fragment of ParB is the major determinant of its ability to form dimers, as deletion of seven amino acids (ParB1-283) or even two amino acids (ParB1-288) impaired significantly the ability of monomers to interact.

ParB$_{P.a.}$ DNA binding *in vitro* (EMSA)

Previous studies (Bartosik *et al*., 2004) indicated that self association of ParB is important for efficient DNA binding (deletion of the C-terminus in ParB1-229 significantly decreased the DNA binding ability but did not completely stop it from binding *parS*). All purified ParB$_{Pa.}$ derivatives were tested for binding to *parS*$_{P.a.}$ using a standard Electrophoretic Mobility Shift Assay (EMSA) (Fig. 2b). Non-radioactive EMSA was performed on *parS* (annealed oligonucleotides #17 and #18) and an unrelated palindrome motif (annealed oligonucleotides #19 and #20) as a control. WT ParB did not bind the control oligonucleotides at tested concentrations. ParBL286A showed affinity towards *parS* approximately two-fold higher than WT ParB whereas ParBV285A and ParBL282A bound *parS* but with 2-fold lower affinity. ParB1-288 and ParB1-283 hardly shifted the ds *parS* oligonucleotides at tested concentrations. Therefore the ability to bind *parS* seems to correlate with the degree of dimerization proficiency as illustrated by comparing panels (a) and (b) in Fig. 2.

ParB$_{P.a.}$ self association and interaction with ParA$_{P.a.}$ *in vivo*

To check the interactions of mutated ParB proteins with WT ParB and ParA *in vivo*, the bacterial adenylate cyclase two-hybrid system in *E. coli* (Karimova *et al*., 1998; 2000) was applied. Mutated ParB derivatives were translationally fused to CyaT18 fragment (pUT18C derivatives), whereas WT ParB and ParA were fused to CyaT25 fragment (pKT25 derivatives). *E. coli* BTH101, an adenylate cyclase deficient strain (*cya*), was co-transformed with a mixture of appropriate pairs of BACTH system plasmids and plated on MacConkey base medium supplemented with 1 % (w/v) maltose, 0.5 mM IPTG and selective antibiotics.

The results of *in vivo* BACTH analysis confirmed the conclusions from the *in vitro* dimerization studies presented above. The two short deletion mutants ParB1-283 and ParB1-288 were unable to associate with WT ParB whereas interactions between ParBL286A and WT ParB were comparable to self-association of WT ParB as demonstrated by BTH101 (pLKB702)(pLKB233) transformants, (Fig. 3). Interactions of ParBL282A and ParBV285A

with WT ParB were weaker than control interactions between pLKB433 and pLKB233 but still very clear. The analysis of interactions of mutant ParB derivatives and ParA showed a correlation between the efficiency of ParB dimerization and the ability to interact with ParA in the BACTH system. ParBL286A demonstrated the interactions with ParA similar to WT ParB. Visibly weaker interactions between ParA and ParBL282A or ParBV285A and no interactions between ParA and ParB1-283 or ParB1-288 were detected. This strongly suggests that the dimer form of ParB is required for interactions with ParA**.**

Introduction of mutant *parB* alleles into the *P. aeruginosa* chromosome

The C-terminal modifications of ParB (ParB1-283 and ParB1-288 as well as ParBL282A and ParBV285A) cause defects in dimerization and in turn defects in DNA binding, transcriptional silencing and interaction with ParA. To determine the phenotypic effect of these mutations all four alleles were introduced into the *P. aeruginosa* chromosome using suicide vector pAKE600 and allele exchange via homologous recombination (El Sayed *et al.*, 2001). The new *P. aeruginosa* PAO1161Rif^R*parB* mutants, *parB1-288* and *parB1-283*, *parB282* and *parB285* were tested for various forms of motility: swimming, swarming and twitching. The drastic defect in swarming, slight defect in swimming and no effect on twitching were observed previously for the *P. aeruginosa* PAO1161Rif^R *parB* null strain (Bartosik *et al.*, 2009). Neither of the new tested mutants was disturbed in twitching (data not shown) but all four were strongly impaired in swarming and slightly affected in swimming (Fig. 4). The *parB282* and *parB285* mutants demonstrated lower defect in swimming when compared to *parB* null, *parB1-288* and *parB1-283* mutants.

To look at the effects of *parB* mutations on *P. aeruginosa* PAO1161Rif^R growth, time course experiments both in rich (L broth) and minimal (M9) medium were conducted. Each growth experiment was performed using cells freshly taken from a deep-frozen stock to reduce the possibility of accumulation of secondary mutations. The new PAO1161Rif^R*parB* mutants (short deletions and single amino acid substitutions) demonstrated the changes in the growth rate comparable to the *parB* null strain. They showed ~10 % longer mean generation time (mgt) in comparison to WT PAO1161Rif^R when grown in L broth or minimal medium (M9) at 37 °C, and ~20 % longer mgt when grown in L-broth at 30 °C (Table 3).

The *parB* mutant strains were also examined for the frequency of anucleate cell formation. Bacterial cells were collected from cultures at late exponential growth phase (OD_{600} 0.8). The cells were fixed and DAPI-stained to visualize chromosomes. The number of cells without chromosomes and the mean cell length were estimated using fluorescence microscopy combined with appropriate software. The frequency of anucleate cell formation

for the *parB* null mutant was more than 100-fold higher than for the wild type strain under the same growth condition on the sample of at least 1000 cells (Table 3). The short C-terminal deletion mutants PAO1161Rif^R*parB1-288, parB1-283* as well as the substitution mutants *parB282* and *parB285* produced anucleate cells at comparable frequency with that observed for the PAO1161Rif^R*parB* null mutant. Measurements of cell length showed that all *parB* mutants produce cells up to 10 % longer on average than those of the wild type similarly to the PAO1161Rif^R*parB* null mutant (Table 3).

In order to check the intracellular concentration of the mutated ParBs, equal numbers of cells of PAO1161Rif^R strain and *parB* mutants from the same growth phases were collected and analyzed by Western blotting with anti-ParB antibodies. The amount of ParBs truncated at the C-terminus was approximately 5-6-fold lower than the amount of WT ParB in actively dividing cells of PAO1161Rif^R strain. A similar decrease was observed for two ParBs with amino acid substitutions at the C-terminus (ParBL282A and ParBV285A) probably due to the lower stability of monomeric ParB (Fig.5a). To exclude the possibility that it was the decreased cellular concentration of ParB rather than the specific mutation that may be responsible for the observed defects in growth and nucleoid segregation, the medium copy broad-host-range plasmid pBBR1-MCS1 carrying the mutated *parB* alleles under control of *tacp* (the plasmid series from pJMB501 to pJMB504) were introduced into the appropriate chromosomal mutants. Western blotting of extracts from defined numbers of cells of such transformants grown in the absence of IPTG showed that the level of mutant ParBs was similar or even higher when related to WT ParB in PAO1161 grown under the same conditions (Fig.5a). The merodiploids strains were also tested for the motilities (Fig.4), growth rate and anucleate cell production (Table 3). No suppression of the defects was observed by increasing production of mutant ParB derivatives, confirming that specific changes in ParB and not a decreased level were responsible for mutant phenotypes.

To visualize the localization and ability of the ParB mutant derivatives to form intracellular foci, immunofluorescence microscopy was applied (Fig. 5b). Fixed cells from exponential phase were first incubated with purified anti-ParB antibodies and then with FITC-conjugated anti-rabbit IgG. Cells of the PAO1161Rif^R*parB* null mutant were also examined as a control for the specificity of the antibodies used. The majority of the actively dividing cells of the wild type strain of *P. aeruginosa* contained from two to four regularly spaced ParB foci as expected from the number of *ori* domains. In cells of mutants *parB1-283*, *parB1-288, parB282* and *parB285* no such strictly organized foci were observed, but instead, multiple irregularly distributed signals appeared in the region of the nucleoid. The

399 fluorescence signals in transformants of the PAO1161Rif^{R}*parB1-283* and
400 PAO1161Rif^{R}*parB1-288* in which truncated ParBs were also supplied from the plasmids
401 formed multiple and dispersed fluorescent foci, similar to those seen in the mutants (data not
402 shown). The diminished ability of ParB derivatives to dimerize conveys into the defect in foci
403 compaction (probably *oriC* domain organization)and nucleoids segregation.
404

DISCUSSION

The work described in this paper adds important details to our understanding of ParB from *P. aeruginosa* which is a key representative of the large family of ParB proteins encoded by both plasmids and chromosomes. Our earlier *in vivo* studies revealed that overproduced ParB of *P. aeruginosa* is able to silence the expression of genes adjacent to the *parS* site (Bartosik *et al.*, 2004) and that spreading activity relies on dimer formation by the C-terminus, DNA binding and N-terminal polymerization domain (Bartosik *et al.*, 2004; Kusiak *et al.*, 2011). Accumulating evidence has shown that this activity is a common feature of ParB family members of Type IA (Bingle *et al.*, 2005; Rodionov *et al*., 1999; Schumacher *et al.*, 2007, 2010), including also the chromosomal homologues (Bartosik *et al.*, 2004; Breier and Grossman, 2007). This silencing is thought to be a consequence of spreading on DNA due to ParB-ParB interactions through the N-terminal polymerization domain (Kusiak *et al*., 2011). However, the physiological role of neither plasmidic (Rodionov and Yarmolinsky, 2004) nor chromosomal ParBs spreading on DNA is clear. The recent studies on Spo0J of *B. subtilis* showed that Spo0J spreads around each *parS* site on chromosomal DNA over dozens of kilo bases (Breier and Grossman, 2007) but under the conditions tested, this process did not significantly affect expression of the majority of genes near *parS*, with the exception of some sporulation genes. The crystallographic studies on ParB homologues of Type IA (Delbruck *et al*., 2002; Khare *et al*., 2004; Leonard *et al*., 2004; Schumacher *et al*., 2007) combined with further experimental verification should help to elucidate the exact role of ParB spreading on DNA and whether this role is universal for all ParB homologues. The discoveries of interactions of chromosomal ParB homologues with DnaA (control of initiation of replication), different proteins involved in chromosome organization and *ori* domain localization (SMC, PopZ, TipN), cytokinesis (FtsZ, MipZ) suggest an important biological role of Par proteins in a wide spectrum of processes, some of them possibly species-specific (Bowman *et al.*, 2008; Donovan et al. 2010; Ebersbach *et al*., 2008; Gruber and Errington, 2009; Kadoya et al., 2011; Murray and Errington, 2008; Ptacin et al., 2010; Schofield et al., 2010; Scholefield et al., 2011; Sullivan *et al.*, 2009; Thanbichler and Shapiro, 2006; Toro *et al.*, 2008). In *P. aeruginosa* ParB seems to be involved not only in the chromosome segregation but also in the control of growth rate, cell motilities and colony morphology (Bartosik et al., 2009). Its role in some but not all of these processes depends on interactions with its cognate ParA counterpart (Kusiak and Jagura-Burdzy, unpublished). It was unclear whether a ParB dimer is required for interactions with ParA and other putative partners. To

correlate the structural information with the physiological role of ParB we looked closely at the C-terminal domain which we had previously established as the dimerization domain of ParB.

Although $ParB_{P.a}$ has not been crystallized yet, the putative three-dimensional structure for the C-terminal (242-290 amino acids) domain of $ParB_{P.a}$ has been predicted, based on crystallographic data for its homologue – KorB protein of plasmid RK2/RP4 (Delbruck *et al*., 2002) (Fig. 1). We constructed five *parB* mutant alleles to define the functionality of proteins modified in C-tip. Both *in vitro* and *in vivo* tests on the ability of ParB derivatives to dimerize indicated that the last two amino acids at the C-terminus within the conserved region 4 are essential for the ability of $ParB_{P.a}$ to self-associate. Removal of I289 and R290 rendered ParB inactive in dimer formation. In agreement with the structural prediction *in silico* two hydrophobic residues L282 and V285 have been confirmed to play a vital role in ParB dimerization. The alanine substitution derivatives ParBL282A and ParBV285A showed detectable changes in self-association in vitro and in association with WT ParB *in vivo*. On the other hand L286, which should be directed outwards from the putative dimer (Fig. 1), has been confirmed experimentally not to be involved in self-associations. The alanine substitution derivative ParBL286A behaved like WT ParB in all tests with the exception of EMSA when it seemed to bind *parS* with even higher affinity than WT ParB.

The four ParB mutant derivatives impaired to various extents in dimerization, were also impaired to similar extents in *parS* binding, strongly implying that ParB binds to *parS* as a dimer. None of these mutants was also able to silence genes adjacent to *parS* suggesting that dimerization through the C-terminus is a prerequisite for spreading on DNA. The necessity of ParB to form dimers before interacting with ParA partner was confirmed by analysis of mutants in the BACTH system. The observed *in vivo* heterologous interactions between ParB mutant derivatives and ParA correlated in strength with the ability of ParB mutants to interact with WT ParB as a dimer.

When these four *parB* alleles were introduced into *P. aeruginosa* chromosome by allele exchange they caused defects in growth rate, motilities (swarming and swimming) and more than 100-fold increase in the frequency of anucleate cell formation. Immunofluorescence microscopy showed that in contrast to WT ParB, which is organized into 1 to 4 regularly distributed foci, the modified ParBs formed multiple smaller foci dispersed within the boundaries of the nucleoid.

It has been noticed that all modified ParBs are present in lower quantities per cell and are more prone to degradation than WT ParB, probably due to inability to be protected by ParA (Lasocki *et al.*, 2007 and Bartosik *et al*., 2009). The elevation of mutant ParBs production to the level observed for WT ParB did not suppress the *parB* mutant phenotypes in the constructed merodiploid strains, suggesting that the decreased level of protein is not the main factor responsible for the visible deficiencies of the mutants.

Despite the fact that ParBs with single amino acid substitution (ParB282 and ParB285) seem to be significantly less impaired in dimerization, DNA binding, or interactions with ParA than the truncated derivatives ParB1-283 and ParB1-288, the phenotypes of four new *parB* mutants were almost identical (with the slight difference between the deletion and point mutants in swimming defects) and they resembled phenotype of *parB* null mutant (Bartosik et al., 2009). Presented data suggests that even small changes in dimerization ability of ParB may transform into lower affinity of *parS* binding and in turn result in inability to spread on DNA (silencing test). And the spreading on DNA has been shown to determine biological function of ParB in *P aeruginosa* (Kusiak *et al*., 2011).

In conclusion, an *in silico* model of the $ParB_{P.a.}$ C-terminal dimerization domain has identified the hydrophobic residues L282 and V285, and charged R290 as vital for dimerization. Substitution of hydrophobic residues by alanine or removal of the two last amino acids I289 and R290 impairs $ParB_{Pa.}$ in dimerization, *parS* binding and ParA interaction and renders it inactive in spreading on DNA (transcriptional silencing). Since such truncation of ParB as well as alanine substitution of two hydrophobic residues lead to the same deficiencies in growth, genome segregation and motilities as complete lack of ParB in *P. aeruginosa* it is clear that dimerization is a vital prerequisite for the function of ParB in the cells.

ACKNOWLEDGEMENTS

This work was funded by Wellcome Trust Collaborative Research Grant Initiative 067068/Z/02/Z, by MNiSW grant 2913/B/PO1/2008/34 and in part by SBM grants 19/2004 and 14/2005 awarded to J. M. We would like to thank Dr Karimova for kindly providing the BACTH system.

REFERENCES

Autret, S., & Errington, J. (2003). A role for division-site-selection protein MinD in regulation of inter nucleoid jumping of Soj (ParA) protein in *Bacillus subtilis*. *Mol Microbiol* **47**, 159-169.

Bartosik, A. A., Lasocki, K., Mierzejewska, J., Thomas, C. M. & Jagura-Burdzy, G. (2004). ParB of *Pseudomonas aeruginosa*: interactions with its partner ParA and its target *parS* and specific effects on bacterial growth. *J Bacteriol* **186,** 6983-6998.

Bartosik, A. A., Mierzejewska, J., Thomas, C. M. & Jagura-Burdzy, G. (2009). ParB deficiency in *Pseudomonas aeruginosa* destabilizes the partner protein ParA and affects a variety of physiological parameters. *Microbiology* **155,** 1080-1092.

Bignell, C. R., Haines, A. S., Khare, D. & Thomas. C. M. (1999). Effect of growth rate and *incC* mutation on symmetric plasmid distribution by the IncP-1 partitioning apparatus. *Mol Microbiol* **34,** 205-216.

Bingle, L. E., Macartney, D. P., Fantozzi, A., Manzoor, S. E. & Thomas, C. M. (2005). Flexibility in repression and cooperativity by KorB of broad host range IncP-1 plasmid RK2. *J Mol Biol* **349,** 302-316.

Bowman, G. R., Comolli, L. R., Zhu, J., Eckart, M., Koenig, M., Downing, K. H., Moerner, W. E., Earnest ,T. & Shapiro, L. (2008). A polymeric protein anchors the chromosomal origin/ParB complex at a bacterial cell pole. *Cell* **134,** 945-955.

Breier, A. M. & Grossman, A. (2007). Whole-genome analysis of the chromosome partitioning and sporulation protein Spo0J (ParB) reveals spreading and origin-distal sites on the *Bacillus subtilis* chromosome. *Mol Microbiol* **64,** 703-718.

Cervin, M. A., Spiegelman, G. B., Raether, B., Ohlsen, K., Perego, M. & Hoch, J. A. (1998). A negative regulator linking chromosome segregation to developmental transcription in *Bacillus subtilis*. *Mol Microbiol* **29,** 85-95.

Churchward, G., Belin, D. & Nagamine, Y. (1984). A pSC101-derived plasmid which shows no sequence homology to other commonly used cloning vectors. *Gene* **31,** 165-171.

Delbrück, H., Ziegelin, G., Lanka, E. & Heinemann, U. (2002). An Src homology 3-like domain is responsible for dimerization of the repressor protein KorB encoded by the promiscuous IncP plasmid RP4. *J Biol Chem* **277,** 4191-4198.

Donovan, C., Schwaiger, A., Krämer, R. & Bramkamp, M. (2010). Subcellular Localization and Characterization of the ParAB System from *Corynebacterium glutamicum*. *J Bacteriol* **192,** 3441-3451.

El-Sayed, A. K., Hothersall, J. & Thomas, C. M. (2001). Quorum-sensing-dependent regulation of biosynthesis of the polyketide antibiotic mupirocin in *Pseudomonas fluorescens* NCIMB 10586. *Microbiology* **147,** 2127-2139.

Ebersbach, G., Briegel, A., Jensen, G. J. & Jacobs-Wagner, C. (2008). A self-associating protein critical for chromosome attachment, division, and polar organization in *Caulobacter*. *Cell* **134,** 956-968.

Figge, R. M., Easter, J. Jr. & Gober, J. W. (2003). Productive interaction between the chromosome partitioning proteins, ParA and ParB, is required for the progression of the cell cycle in *Caulobacter crescentus*. *Mol Microbiol* **47,** 1225-1237.

Fogel, M. A. & Waldor, M. K. (2006). A dynamic, mitotic-like mechanism for bacterial chromosome segregation. *Genes Dev* **20,** 3269-3282.

Gerdes, K., Møller-Jensen, J. & Jensen, R. B. (2000). Plasmid and chromosome partitioning: surprises from phylogeny. *Mol Microbiol* **37,** 455-466.

Glaser, P., Sharpe, M.E., Raether, B., Perego, M., Ohlsen, K. & Errington, J. (1997). Dynamic, mitotic-like behavior of a bacterial protein required for accurate chromosome partitioning. *Genes Dev* **11**, 1160-1168.

Godfrin-Estevenon, A.-M., Pasta, F. & Lane, D. (2002). The *parAB* gene products of *Pseudomonas putida* exhibit partition activity in both *P. putida* and *Escherichia coli*. *Mol Microbiol* **43,** 39-49.

Gruber, S. & Errington, J. (2009). Recruitment of condensin to replication origin regions by ParB/SpoOJ promotes chromosome segregation in *B. subtilis*. *Cell* **137,** 685-696.

Irani, V. R., & Rowe, J. J. (1997). Enhancement of transformation in *Pseudomonas aeruginosa* PAO1 by Mg^{2+} and heat. *BioTechniques* **22,** 54-56.

Ireton, K., Gunther, N. W. 4th & Grossman, A. D. (1994). *spo0J* is required for normal chromosome segregation as well as the initiation of sporulation in *Bacillus subtilis*. *J Bacteriol* **176**, 5320-5329.

Jagura-Burdzy, G. & Thomas, C. M. (1995). Purification of KorA protein from broad host range plasmid RK2: definition of a hierarchy of KorA operators. *J Mol Biol* **253,** 39-50.

Jakimowicz, D., Chater, K. F. & Zakrzewska-Czerwinska, J. (2002). The ParB protein of *Streptomyces coelicolor* A3(2) recognizes a cluster of *parS* sequences within the origin-proximal region of the linear chromosome. *Mol Microbiol* **45,** 1365-1377.

Jakimowicz, D., Mouz, S., Zakrzewska-Czerwinska, J. & Chater, K. F. (2006). Developmental control of a *parAB* promoter leads to formation of sporulation-associated ParB complexes in *Streptomyces coelicolor*. *J Bacteriol* **188,** 1710-1720.

Jakimowicz, D., Zydek, P., Kois, A., Zakrzewska-Czerwińska, J. & Chater, K. F. (2007). Alignment of multiple chromosomes along helical ParA scaffolding in sporulating *Streptomyces* hyphae. *Mol Microbiol* **65,** 625-641.

Kadoya, R., Baek, J. H., Sarker A. & Chattoraj, D. K. (2011). Participation of chromosome segregation protein ParAI of *Vibrio cholerae* in chromosome replication. *J Bacteriol* **193**, 1504-1514.

Kahn, M. R., Kolter, R., Thomas, C. M., Figurski, D., Meyer, R., Remault, E. & Helinski, D. R. (1979). Plasmid cloning vehicles derived from plasmids ColE1, F, R6K, and RK2. *Methods Enzymol* **68**, 268-280.

Karimova, G., Pidoux, J., Ullmann, A. & Ladant, D. (1998). A bacterial two-hybrid system based on a reconstituted signal transduction pathway. *Proc Natl Acad Sci U S A* **95,** 5752-5756.

Katoh, K. & Toh, H. (2008). Recent developments in the MAFFT multiple sequence alignment program. *Brief Bioinform* **9,** 286-298.

Khare, D., Ziegelin, G., Lanka, E. & Heinemann, U. (2004). Sequence-specific DNA binding determined by contacts outside the helix-turn-helix motif of the ParB homolog KorB. *Nat Struct Mol Biol* **11,** 656-663.

Kim, H.-J, Calcut, M. J., Schmidt, F. J. & Chater, K. F. (2000). Partitioning of the linear chromosome during sporulation of *Streptomyces coelicolor* A3(2) involves an *oriC*-linked *parAB* locus. *J Bacteriol* **182,** 1313-1320.

Kovach, M. E., Elzer, P. H., Hill, D. S., Robertson, G. T., Farris, M. A., Roop, R. M. 2nd & Peterson, K. M. (1995). Four new derivatives of the broad-host-range cloning vector pBBR1MCS1, carrying different antibiotic- resistance cassettes. *Gene* **166,**175-176.

Kusiak, M., Gapczynska, A., Plochocka, D., Thomas, C. M. & Jagura-Burdzy, G. (2011). Binding and spreading of ParB on DNA determine its biological function in *Pseudomonas aeruginosa*. *J Bacteriol* **193,** 3342-3355.

Larkin, M. A., Blackshields, G., Brown, N. P., Chenna, R., McGettigan, P. A., McWilliam, H., Valentin, F., Wallace, I. M., Wilm, A. & other authors. (2007). Clustal W and Clustal X version 2.0. *Bioinformatics* **23,** 2947-2948.

Lasocki, K., Bartosik, A. A., Mierzejewska, J., Thomas, C. M. & Jagura-Burdzy, G. (2007). Deletion of the *parA* (*soj*) homologue in *Pseudomonas aeruginosa* causes ParB

603 instability and affects growth rate, chromosome segregation, and motility. *J Bacteriol* **189,**
604 5762-5772.
605 **Lee, P. S. & Grossman, A. D. (2006).** The chromosome partitioning proteins Soj (ParA) and
606 Spo0J (ParB) contribute to accurate chromosome partitioning, separation of replicated sister
607 origins, and regulation of replication initiation in *Bacillus subtilis*. *Mol Microbiol* **60**, 853-
608 869.
609 **Lee, P. S., Lin, D. C.-H., Moriya, S. & Grossman, A. D. (2003).** Effects of the chromosome
610 partitioning protein Spo0J (ParB) on *oriC* positioning and replication initiation in *Bacillus*
611 *subtilis*. *J Bacteriol* **185,** 1326-1337.
612 **Leonard, T. A., Butler, P. J. & Löwe, J. (2004).** Structural analysis of the chromosome
613 segregation protein Spo0J from *Thermus thermophilus*. *Mol Microbiol* **53,** 419-432.
614 **Lewis, R. A., Bignell, C. R., Zeng, W., Jones, A. C. & Thomas, C. M. (2002).**
615 Chromosome loss from *par* mutants of *Pseudomonas putida* depends on growth medium and
616 phase of growth. *Microbiology* **148,** 537-548.
617 **Lin, D. C.-H. & Grossman, A. D. (1998).** Identification and characterization of a bacterial
618 chromosome partitioning site. *Cell* **92,** 675-685.
619 **Marston, A. L. & Errington, J. (1999).** Dynamic movement of the ParA-like Soj protein of
620 *B. subtilis* and its dual role in nucleoid organization and developmental regulation. *Mol Cell*
621 **4,** 673-682.
622 **Mohl, D. A., Easter, J. Jr. & Gober, J. W. (2001).** The chromosome partitioning protein,
623 ParB, is required for cytokinesis in *Caulobacter crescentus*. *Mol Microbiol* **42,** 741-755.
624 **Mohl, D. A. & Gober, J. W. (1997).** Cell-cycle dependent polar localization of chromosome
625 partitioning proteins in *Caulobacter crescentus*. *Cell* **88,** 675-684.
626 **Mullis, K., Faloona, F. , Scharf, S., Saiki, R., Horn, G. & Erlich, H. (1986).** Specific
627 enzymatic amplification of DNA *in vitro*: the polymerase chain reaction. *Cold Spring Harbor*
628 *Symp. Quant Biol* **51,** 263-273.
629 **Murray, H. & Errington, J. (2008).** Dynamic control of the DNA replication initiation
630 protein DnaA by Soj/ParA. *Cell* 135, 74–84.
631 **Notredame, C., Higgins, D. G. & Heringa, J. (2000).** T-Coffee: A novel method for fast and
632 accurate multiple sequence alignment. *J Mol Biol* **302,** 205-217.
633 **Ogura, Y., Ogasawara, N., Harry, E. J. & Moriya, S. (2003).** Increasing the ratio of Soj to
634 Spo0J promotes replication initiation in *Bacillus subtilis*. *J Bacteriol* **185,** 6316-6324.

635 **Quisel, J. D. & Grossman, A. D. (2000).** Control of sporulation gene expression in *Bacillus*
636 *subtilis* by the chromosome partitioning proteins Soj (ParA) and Spo0J (ParB). *J Bacteriol*
637 **182,** 3446-3451.
638 **Quisel, J. D., Lin, D. C. & Grossman, A. D. (1999).** Control of development by altered
639 localization of a transcription factor in *B. subtilis*. *Mol Cell* **4,** 665-672.
640 **Ptacin, J. L., Lee, S. F., Garner, E. C., Toro, E., Eckart, M., Comolli, L. R., Moerner, W.**
641 **E. & Shapiro, L. (2010).** A spindle-like apparatus guides bacterial chromosome segregation.
642 *Nat Cell Biol* **12,** 791-798.
643 **Rashid, M. H. & Kornberg, A. (2000).** Inorganic polyphosphate is needed for swimming,
644 swarming, and twitching motilities of *Pseudomonas aeruginosa*. *Proc Natl Acad Sci U S A*
645 **97,** 4885-4890.
646 **Real, G., Autret, S., Harry, E.J., Errington, J. & Henriques, A.O. (2005).** Cell division
647 protein DivIB influences the Spo0J/Soj system of chromosome segregation in *Bacillus*
648 *subtilis*. *Mol Microbiol* **55,** 349-367.
649 **Rodionov, O., Lobocka, M. & Yarmolinsky, M. (1999).** Silencing of genes flanking the P1
650 plasmid centromere. *Science* **283,** 546-549.
651 **Rodionov O. & Yarmolinsky, M. (2004).** Plasmid partitioning and the spreading of P1
652 partition protein ParB. *Mol. Microbiol.* **52**, 1215-1223.
653 **Saint-Dic, D., Frushour, B. P., Kehrl, J. H. & Kahng, L. S. (2006).** A *parA* homolog
654 selectively influences positioning of the large chromosome origin in *Vibrio cholerae*. *J*
655 *Bacteriol* **188,** 5626-5631.
656 **Sambrook, J., Fritsch, E. F. & Maniatis, T. (1989).** Molecular cloning: a Laboratory
657 Manual, 2nd edn. Cold Spring Harbor, NY: Cold Spring Harbor Laboratory.
658 **Schofield, W. B., Lim, H. Ch. & Jacobs-Wagner, C. (2010).** Cell cycle coordination and
659 regulation of bacterial chromosome segregation dynamics by polarly localized proteins.
660 *EMBO J* **29,** 3068–3081.
661 **Scholefield, G., Whiting, R., Errington, J. & Murray, H. (2011).** Spo0J regulates the
662 oligomeric state of Soj to trigger its switch from an activator to an inhibitor of DNA
663 replication initiation. *Mol Microbiol* **79,** 1089-1100.
664 **Schumacher, M. A., Mansoor, A. & Funnell, B. E. (2007).** Structure of a four-way bridged
665 ParB-DNA complex provides insight into P1 segrosome assembly. *J Biol Chem* **282,** 10456-
666 10464.

Schumacher, M. A., Piro, K. M. & Xu, W. (2010). Insight into F plasmid DNA segregation revealed by structures of SopB and SopB-DNA complexes. *Nucleic Acids Res* **38,** 4514-4526.

Sharpe, M. E. & Errington, J. (1996). The *Bacillus subtilis soj-spo0J* locus is required for a centromere-like function involved in prespore chromosome partitioning. *Mol Microbiol* **21,** 501-509.

Simon , R., O'Connell, M., Labes, M. & Puhler, A. (1986). Plasmid vectors for the genetic analysis and manipulation of *Rhizobia* and other gram-negative bacteria. *Methods Enzymol* **118,** 640-659.

Sullivan, N. L., Marquis, K. A. & Rudner, D. Z. (2009). Recruitment of SMC by ParB-*parS* organizes the origin region and promotes efficient chromosome segregation. *Cell* **137,** 697-707.

Thanbichler, M. & Shapiro, L. (2006). MipZ, a spatial regulator coordinating chromosome segregation with cell division in *Caulobacter*. *Cell* **126,** 147-162.

Toro, E., Hong, S-H., McAdams, H. H. &Shapiro, L.,(2008). *Caulobacter* requires a dedicated mechanism to initiate chromosome segregation. *Proc Natl Acad Sci U S A* **105,** 15435-15440.

Viollier, P., Thanbichler, M., McGrath, P. T., West, L., Meewan, M., McAdams, H. H. & Shapiro, L. (2004). Rapid and sequential movement of individual chromosomal loci to specific subcellular locations during bacterial DNA replication. *Proc Natl Acad Sci U S A* **101,** 9257-9262.

Webb, C. D., Teleman, A., Gordon, S., Straight, A., Belmont, A., Lin, D. C.-H., Grossman, A. D., Wright, A. & Losick, R. (1997). Bipolar localization of the replication origin regions of chromosomes in vegetative and sporulating cells of *B. subtilis*. *Cell* **88,** 667–674.

Williams, D. R. & Thomas, C. M. (1992). Active partitioning of bacterial plasmids. *J Gen Microbiol* **138,** 1-16.

Yamaichi, Y. & Niki, H. (2000). Active segregation by the *Bacillus subtilis* partitioning system in *Escherichia coli*. *Proc Natl Acad Sci U S A* **97,** 14656-14661.

Figure legends

Fig. 1. Model of a dimer of C-termini $ParB_{P.a}$ (242-290 amino acids). The mutagenized residues are shown as sticks in the red subunit (labeled according to their position in $ParB_{P.a.}$ sequence). The indicated residues L282 and V285 in grey subunit are possibly involved in a leucine zipper formation. The distance between R290 of one monomer and Q266 of another facilitates the electrostatic interactions (magnification at the left site).

Fig. 2. $ParB_{Pa}$ self-association and DNA binding *in vitro*.

(a) Cross-linking with glutaraldehyde (GA) of ParB variants. Purified His_6-tagged proteins at a concentration of 0.1 mg ml^{-1} were incubated at room temperature for 20 minutes without (0) or with increasing concentrations (1×, 2×, 5×, 10×10^{-3} %) of glutaraldehyde. The samples were separated by SDS-PAGE on 12 % gels and analyzed by Western blotting with anti-ParB antibodies. Monomeric, dimeric and higher forms are indicated by m, d and h, respectively.

(b) DNA binding affinity of ParB derivatives (EMSA). Purified His_6-tagged proteins (10, 20, 30, 50 pmoles) were incubated with 5.6 pmoles of ds $parS_{Pa}$ oligonucleotide at 37 °C for 15 minutes. As a control ds oligonucleotides with an unrelated palindromic motif were used under the same conditions.

Fig. 3. Heterodimer formation of ParB variants with WT ParB and ParA *in vivo* (BACTH). Double transformants of *E. coli* BTH101(pLKB4 derivatives)(pLKB2 derivatives) were streaked on MacConkey indicator medium supplemented with penicillin, kanamycin and 0.5. mM IPTG to visualize protein interactions. Dark streaks are indicative of interaction between the two proteins, whereas light ones correspond to a lack of interaction.

Fig. 4. Motility assays for *P. aeruginosa* PAO1161 Rif^R, *parB* mutants and merodiploid strains. Volume-standardized plates for swarming and swimming were inoculated with a sterile toothpick using material from a single colony and incubated for 24 h at 30 ºC. The zones of growth/spreading are indicated in millimeters, the boundaries of the swimming zones are marked by arrows.

Fig. 5. The effect of ParB modifications on its turnover and cellular localization.

(a) Intracellular levels of ParB in *P. aeruginosa* PAO1161 Rif^R pBBR1-MCS, *parB* mutants with pBBR1-MCS and merodiploids of *parB* mutants with the appropriate mutant allele on the pBBR1-MCS under control of *tacp*. Total cellular extracts from 1×10^9 cells were

separated on SDS-PAGE and analyzed by Western blot with anti-ParB antibodies. His-tagged purified ParB was run on the gel as a control. Two cultures of all merodiploid strains were analyzed. The intensities of signals were estimated using ImageQuant and shown underneath as relative (%) to the values obtained for WT strain. **(b)** Immunofluorescence/phase contrast overlaid images showing ParB localization in cells of *P. aerugionosa* PAO1161Rif^{R}*parB* mutants. Cells from the exponential growth phase (OD_{600} 0.5), grown on L broth at 37 °C, were fixed. The dark background is a phase contrast image, blue color shows DAPI-stained chromosome, green color indicates FITC-stained $ParB_{P.a.}$.

740 **Table 1.** List of plasmids used in this work

Designation	Relevant features	Reference or the source
plasmids provided by others:		
pABB811	pGB2 with *parS*$_{2/3}$ sequence (orientation I)	Bartosik *et al.*, 2004
pAKE600	*ori*$_{MB1}$, *oriT*$_{RK2}$, Ap^R, *sacB*	El Sayed *et al.*, 2001
pET28mod	*ori*$_{MB1}$, Km^R, T7*p*, *lacO*, His tag, no BamHI site, T7 tag deleted	Jagura-Burdzy, G.
pBBR1MCS	IncA/C broad-host-range cloning vector, *lacZα*-MCS, *mob*, T7*p*, T3*p*, Cm^R	Kovach *et al.*, 1995
pGB2	*ori*$_{SC101}$, Sp^R/Sm^R, *repA* gene downstream of MCS	Churchward *et al.*, 1984
pGBT30	*ori*$_{MB1}$, Ap^R, *lacI*^{Q}, *tacp* expression vector	Jagura-Burdzy *et al.*, 1991
pGEM-T Easy	*ori*$_{MB1}$, Ap^R	Promega
pJMB500	pBBR1MCS with *lacI*^{Q} *tacp-parB*	Lasocki *et al.*, 2007
pKLB2	pGBT30 with *tacp-parB*	Bartosik *et al.*, 2004
pKLB2.8	pET28mod with T7*p-parB*	Bartosik *et al.*, 2004
pKT25	*ori*$_{p15}$, Km^R, *lacp-cya*T25	Karimova, G.
pKT25-zip	derivative of pKT25 in which the leucine zipper of GCN4 is translationally fused with *cya*T25 fragment	Karimova, G.
pLKB2	pKT25 modified in MCS	Kusiak, L.
pLKB220	pLKB2 with translationally fused *cya*T25-*parA*	Kusiak, L.
pLKB233	pLKB2 with translationally fused *cya*T25-*parB*	Kusiak, L.
pLKB4	pUT18C modified in MCS	Kusiak, L.
pLKB433	pLKB4 with translationally fused *cya*T18-*parB*	Kusiak, L.
pUT18C	*ori*$_{ColE1}$, Ap^R, *lacp-cya*T18	Karimova, G.
pUT18C-zip	derivative of pUT18C in which the leucine zipper of GCN4 is translationally fused with *cya*T18 fragment	Karimova, G.
plasmids constructed during this work:		
pGEM-T Easy derivatives with inserted PCR products		
pJMB26	*parB1-288* allele PCR amplified using #1 and #4 primers	
pJMB27	*parB1-283* allele PCR amplified using #1 and #5 primers	
pJMB28	379 bp fragment PCR amplified using #11 and #12 primers	
pET28mod derivatives		
pJMB100	pKLB2.8 derivative T7-*parB282* (site-directed mutagenesis with pair of primers #21 and #22 to introduce substitution L282A into ParB)	
pJMB101.1	pKLB2.8 derivative T7-*parB285* (site-directed mutagenesis with pair of primers #23 and #24 to introduce substitution V285A into ParB)	
pJMB102	pKLB2.8 derivative T7-*parB286* (site-directed mutagenesis with pair of primers #25 and #26 to introduce substitution L286A into ParB)	
pMMB5.2	pKLB2.8 derivative T7- *parB1-288* (the EcoRI-SalI fragment of pJMB26)	
pMMB6.2	pKLB2.8 derivative T7- *parB1-283* (the EcoRI-SalI fragment of pJMB27)	
pAKE600 derivatives (suicide vector for gene exchange)		
pJMB400	the EcoRI-SalI fragment of pMMB5.2 carrying *parB1-288*	
pJMB401	the EcoRI-SalI fragment of pMMB6.2 carrying *parB1-283*	
pJMB402	the 379 bp SalI - BamHI fragment of pJMB28 inserted into pJMB400	
pJMB403	the 379 bp SalI - BamHI fragment of pJMB28 inserted into pJMB401	

pJMB404	the EcoRI-SalI fragment of pJMB100 carrying *parB282*
pJMB405	the EcoRI-SalI fragment of pJMB101.1 carrying *parB285*
pJMB406	the 379 bp SalI - BamHI fragment of pJMB28 inserted into pJMB404
pJMB407	the 379 bp SalI - BamHI fragment of pJMB28 inserted into pJMB405
pBBR1MCS1 derivatives	
pJMB501	the BamHI-SalI fragment of pJMB604 carrying *lacI*^{Q} and *tacp- parB1-283* transcriptional fusion
pJMB502	the BamHI-SalI fragment of pJMB603 carrying *lacI*^{Q} and *tacp- parB1-288* transcriptional fusion
pJMB503	the BamHI-SalI fragment of pJMB600 carrying *lacI*^{Q} and *tacp- parB282* transcriptional fusion
pJMB504	the BamHI-SalI fragment of pJMB601.1 carrying *lacI*^{Q} and *tacp- parB285* transcriptional fusion
pGBT30 derivatives	
pJMB600	the EcoRI-SalI fragment of pJMB100 to form a *tacp-parB282* transcriptional fusion
pJMB601.1	pKLB2 derivative *tacp-parB285* (PCR site-directed mutagenesis with pair of primers #23 and #24 to introduce V285A substitution into ParB)
pJMB602	the EcoRI-SalI fragment of pJMB102 to form a *tacp-parB286* transcriptional fusion
pJMB603	the EcoRI-SalI fragment of pJMB26 to form a *tacp-parB1-288* transcriptional fusion
pJMB604	the EcoRI-SalI fragment of pJMB27 to form a *tacp-parB1-283* transcriptional fusion
BACTH system plasmids (pUT18C derivatives)	
pJMB700	the EcoRI–HincII fragment of pJMB100 inserted into pLKB4 between restriction sites EcoRI and SmaI to create *cya*T18-*parB282* translational fusion
pJMB701.1	the EcoRI–HincII fragment of pJMB101.1 inserted into pLKB4 between restriction sites EcoRI and SmaI to create *cya*T18-*parB285* translational fusion
pJMB702	the EcoRI–HincII fragment of pJMB102 inserted into pLKB4 between restriction sites EcoRI and SmaI to create *cya*T18-*parB286* translational fusion
pJMB703	the EcoRI–HincII fragment of pMMB5.2 inserted into pLKB4 between restriction sites EcoRI and SmaI to create *cya*T18-*parB1-288* translational fusion
pJMB704	the EcoRI–HincII fragment of pMMB6.2 inserted into pLKB4 between restriction sites EcoRI and SmaI to create *cya*T18-*parB1-283* translational fusion

741

742

743

744 **Table 2.** Transformation frequencies of DH5α(pABB811*parS*) strain with plasmids
745 over-expressing various $parB_{P.a.}$ alleles.

plasmid used for transformation	*selection plates*		
	L agar + **Pn** [a]	L agar + **Pn Sm** [a]	L agar + **Pn Sm IPTG** [a]
pGBT30 (vector)	4.47×10^4	3.90×10^4	4.07×10^4
pKLB2 (wt *parB*)	2.40×10^3	9.00×10^2	< 10
pJMB600 (*parB282*)	8.60×10^3	5.80×10^3	3.50×10^3
pJMB601.1 (*parB285*)	2.18×10^4	9.70×10^3	6.80×10^3
pJMB602 (*parB286*)	1.30×10^3	5.00×10^2	< 10
pJMB603 (*parB1-288*)	1.20×10^4	4.80×10^3	4.10×10^3
pJMB604 (*parB1-283*)	4.30×10^3	1.80×10^3	1.50×10^3

746 [a]The experiments were repeated three times, the same pattern of ”silencing” was observed.

747
748

Table 3. Phenotypes of PAO1161Rif^R*parB* mutants.

***parB* allele**	**division time [min][a]**			**anucleate cells [%][b]**	**mean cell length [µm][c]**
	L broth 37 °C	L broth 30 °C	M9 37 °C		
parB1-283	32 ± 1	54 ± 5	119 ± 10	1.8	1.9 ± 0.4
parB1-283/ pJMB501	32 ± 1	nd	nd	1.6	1.9 ± 0.4
parB1-288	32 ± 1	55 ± 5	122 ± 11	1.3	1.8± 0.4
parB1-288/ pJMB502	32 ± 1	nd	nd	1.3	1.8 ± 0.4
parB282	32 ± 1	52± 5	120± 10	2.2	1.9 ± 0.5
parB282/ pJMB503	nd	nd	nd	2.6	1.9 ± 0.5
parB285	32 ± 1	58± 5	125± 10	2.2	1.8 ± 0.4
parB285/ pJMB504	nd	nd	nd	3.6	1.8 ± 0.5
parB null	33 ± 2	54 ± 4	125 ± 11	2.1	1.9 ± 0.5
wild-type	30 ± 1	46 ± 3	110± 10	< 0.01	1.6 ± 0.4

[a] Division time in minutes at different growth conditions, data from three independent experiments; [b] and [c] estimated by DAPI staining and microscopic observations. Data from at least 1000 cells.

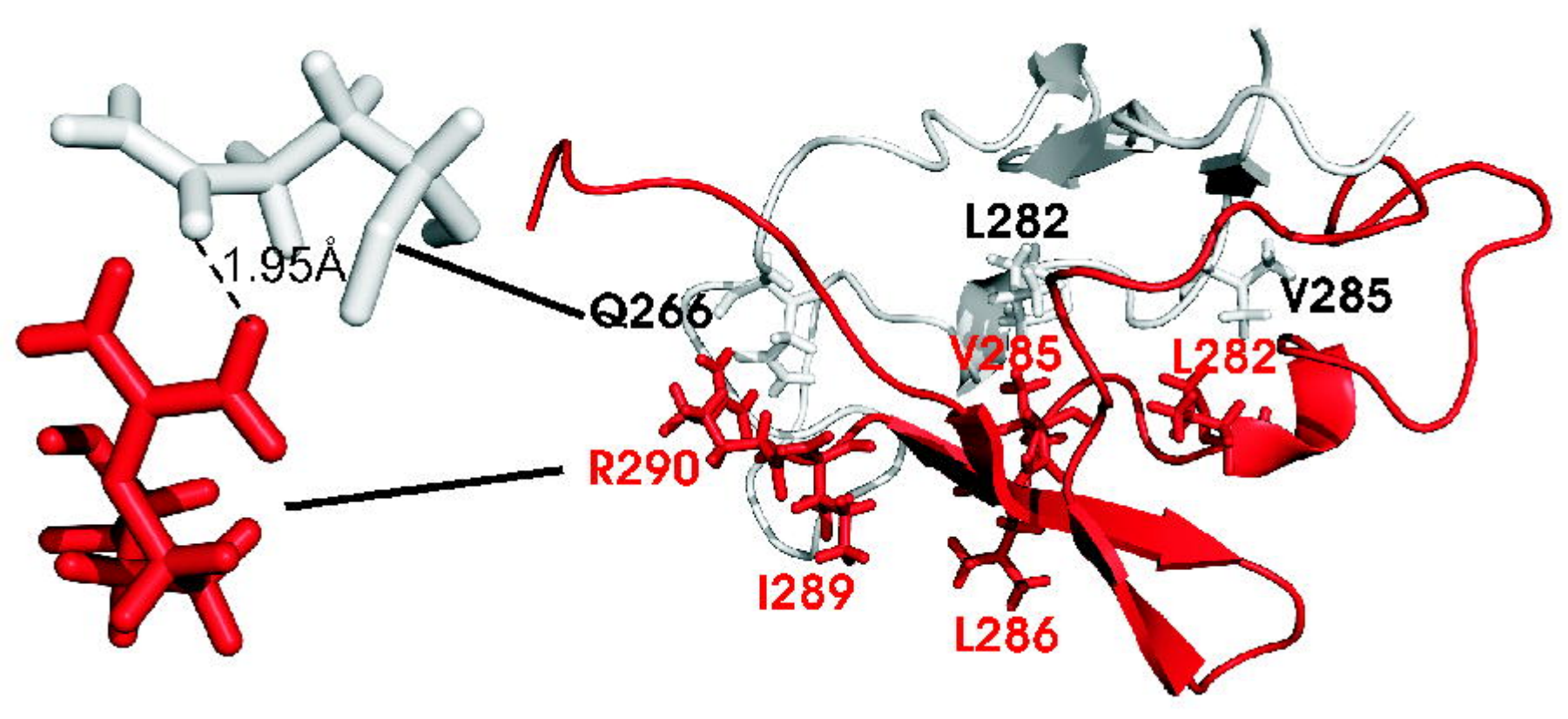
1.95Å
Q266
L282
V285
V285
L282
R290
I289
L286

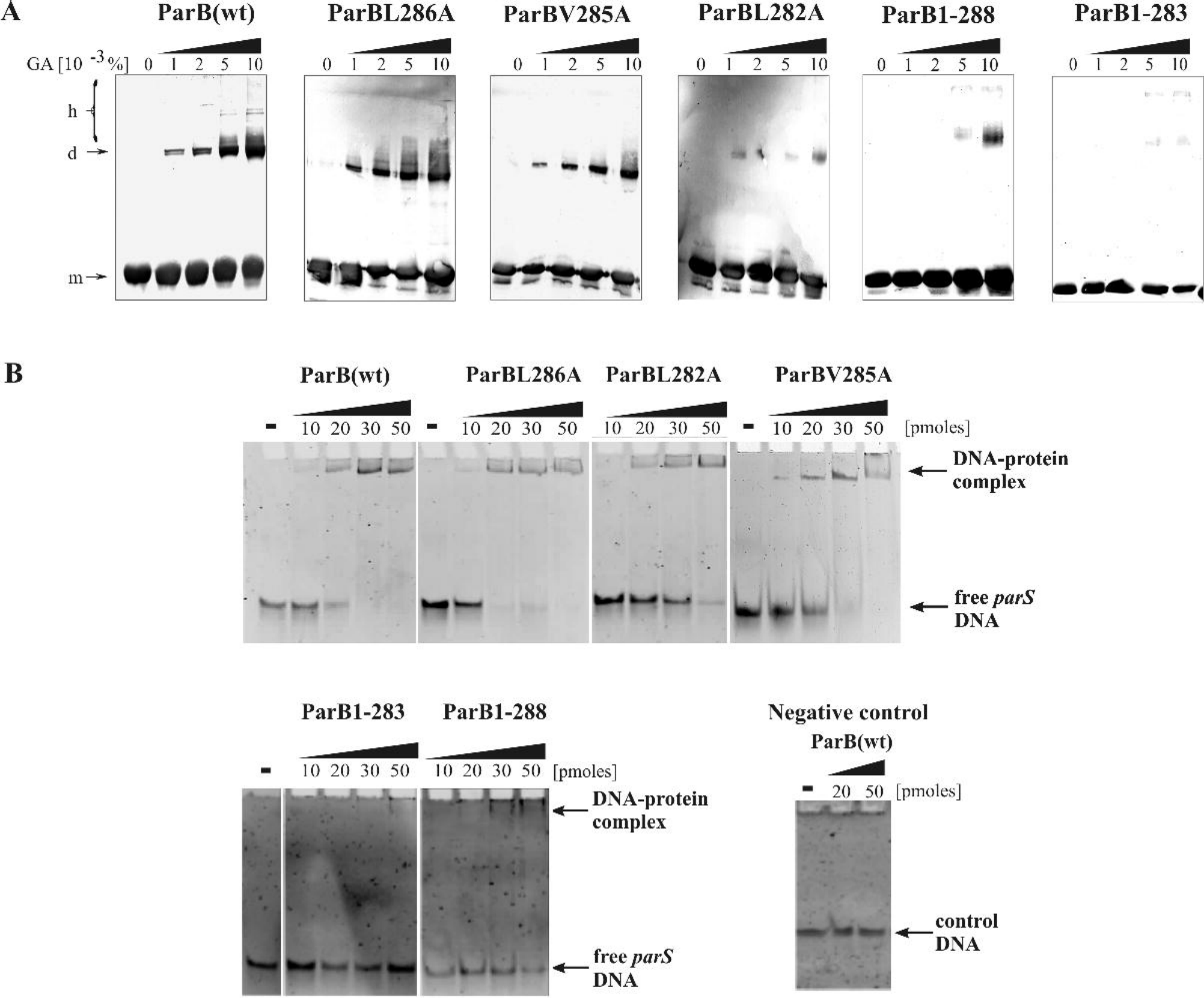
A
ParB(wt)
ParBL286A
ParBV285A
ParBL282A
ParB1-288
ParB1-283
GA [10 -3 %]
0 1 2 5 10
h
d
m
B
ParB(wt)
ParBL286A
ParBL282A
ParBV285A
- 10 20 30 50
[pmoles]
DNA-protein complex
free parS DNA
ParB1-283
ParB1-288
Negative control
ParB(wt)
- 20 50 [pmoles]
control DNA

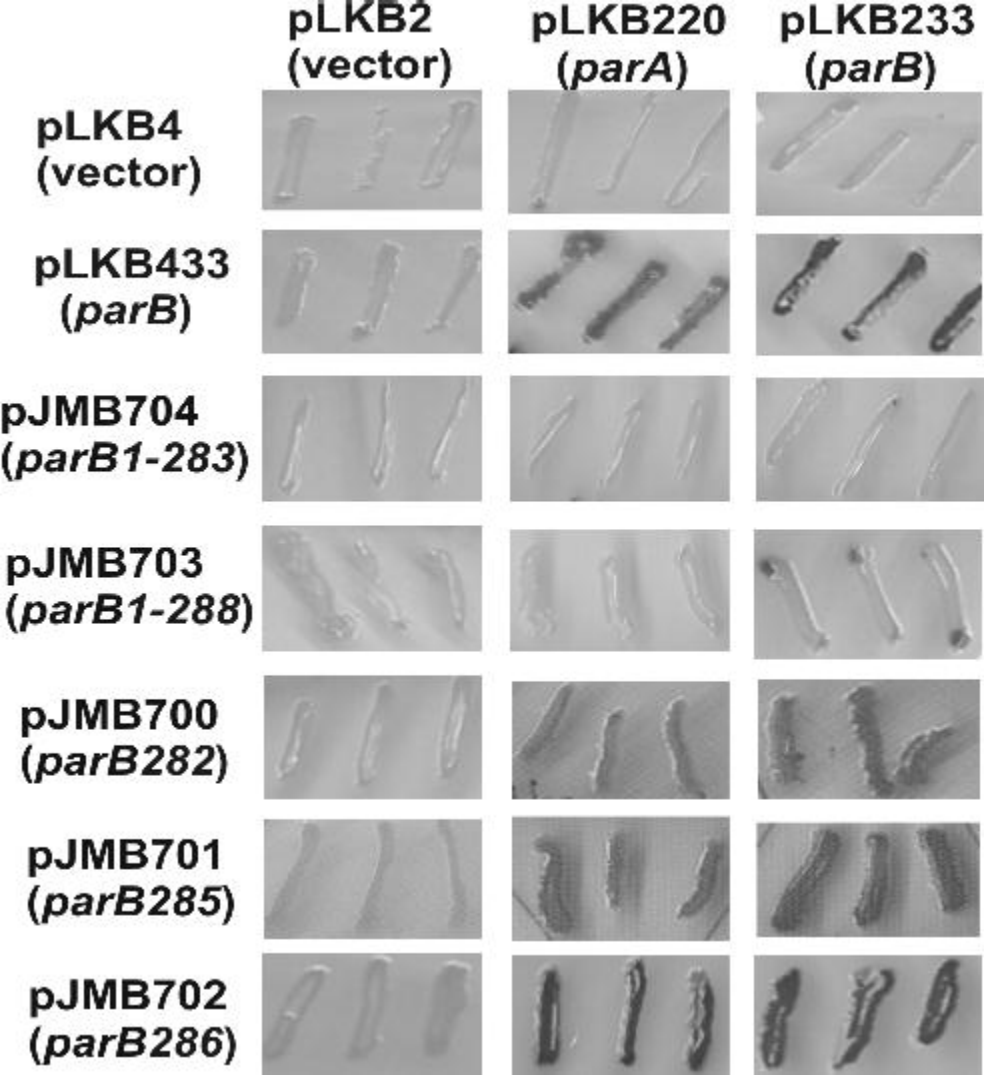
pLKB2 (vector)
pLKB220 (parA)
pLKB233 (parB)
pLKB4 (vector)
pLKB433 (parB)
pJMB704 (parB1-283)
pJMB703 (parB1-288)
pJMB700 (parB282)
pJMB701 (parB285)
pJMB702 (parB286)

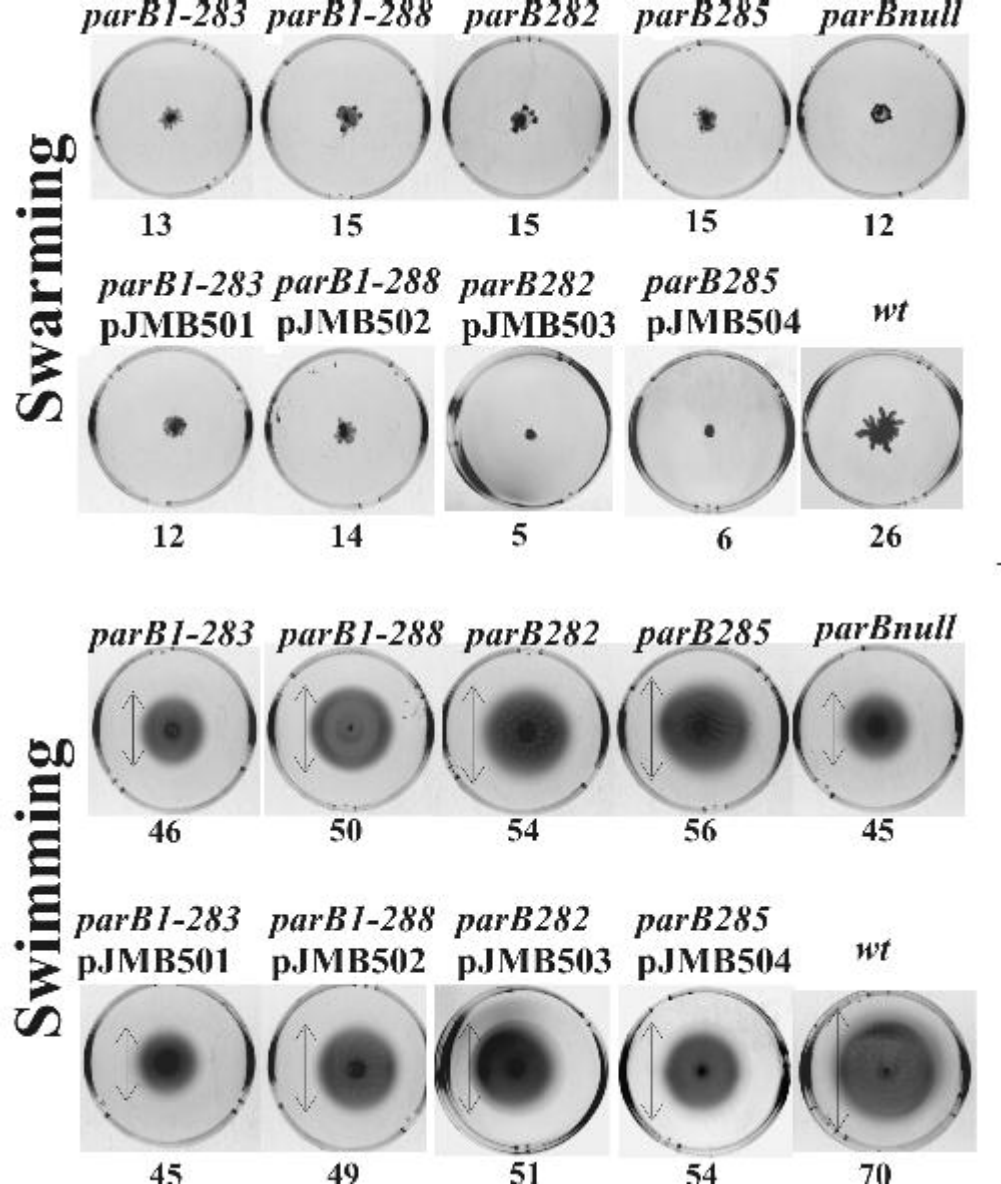
Swarming
parB1-283
parB1-288
parB282
parB285
parBnull
13
15
15
15
12
parB1-283 pJMB501
parB1-288 pJMB502
parB282 pJMB503
parB285 pJMB504
wt
12
14
5
6
26
Swimming
parB1-283
parB1-288
parB282
parB285
parBnull
46
50
54
56
45
parB1-283 pJMB501
parB1-288 pJMB502
parB282 pJMB503
parB285 pJMB504
wt
45
49
51
54
70

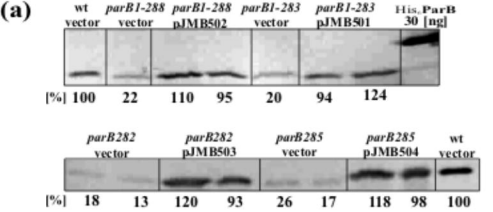
(a)
wt vector
parB1-288 vector
parB1-288 pJMB502
parB1-283 vector
parB1-283 pJMB501
His6ParB 30 [ng]
[%] 100 22 110 95 20 94 124
parB282 vector
parB282 pJMB503
parB285 vector
parB285 pJMB504
wt vector
[%] 18 13 120 93 26 17 118 98 100

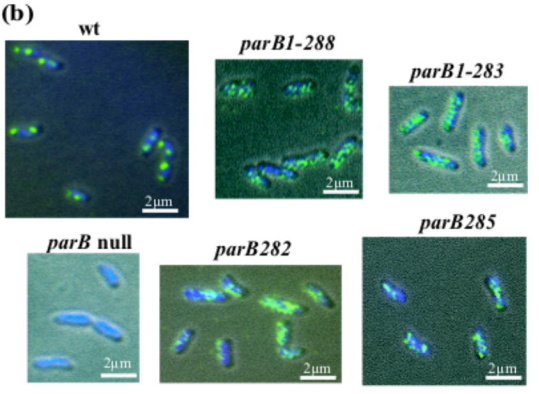
(b)
wt
parB1-288
parB1-283
parB null
parB282
parB285
2µm

Figure 5